

## The role of Coulomb fields in the formation of emittance in photoguns

© V.Ya. Ivanov, A.E. Levichev

G.I. Budker Institute of Nuclear Physics, Siberian Branch of the Russian Academy of Sciences,  
630090 Novosibirsk, Russia e-mail: vivanov.48@mail.ru

Received May 29, 2022

Revised December 2, 2022

Accepted July 13, 2023

A theoretical analysis is made of the formation of longitudinal and transverse emittance of beams of charged particles in photoguns under the influence of repulsive forces of Coulomb fields. In numerical calculations, the characteristics of bunches of charged particles with uniform and Gaussian charge density distributions are compared. The efficiency of the proposed numerical-analytical model is compared with calculations using the Astra program. The obtained numerical and analytical results can be useful in the design of photoinjectors to select the optimal parameters that determine the main characteristics of photoguns.

**Keywords:** coulomb fields, photoguns, bundles, emittance.

DOI: 10.61011/TP.2023.09.57355.147-23

### Introduction

Modern accelerators require the use of high quality electron beams. In projects such as SKEKB [1,2], FCC [3], or Super C-Tau Factory [4], it is necessary to form particle clumps with a charge of 1–6.5 nC, an energy spread of less than 1%, and a normalized transverse emittance of less than 20 mm·mrad. Electron guns with a thermo-cathode can generate beams with the desired current, but achieving low emittance and energy spread presents great difficulties. For example, when using S-band accelerating structures, the slot length should be a few millimeters with an energy spread of less than 1%. FCC or Super C-Tau Factory projects require an energy spread of 0.1% or less, so the slot length should be less than 1 mm. With these requirements, the use of thermal cathode guns with high beam compression poses a significant challenge.

HF guns with metal or semiconductor photocathodes seem to be more promising in this respect. Such photocathodes make it possible to generate particle clots with a length equal to the laser pulse duration, i.e. less than 1 ps. These guns provide a high rate of acceleration, resulting in particles with relativistic energies at a short distance from the cathode. All this makes it possible to achieve a small value of transverse emittance. The disadvantage of photocannon with a metal photocathode is the small value of quantum efficiency, but the achievements of recent years have led to an improvement of the situation with this parameter, which is associated, in particular, with the transition to semiconductor cathodes.

Despite the advances in photocannon design, there are many problems to be solved. One of them is the high charge of the clot, which makes it difficult to produce a beam with low emittance. Since 1985 when the first photogun was designed at Los Alamos Laboratory, such beam sources have become increasingly popular. Photocannons are capable of generating beams with small

transverse emittance [5–9]. In addition, they allow to obtain high current density compared to traditional thermionic guns, achieve high beam brightness [10]. This becomes possible because the charged particle cluster initiated by the laser pulse immediately finds itself in the field of a resonant cavity with a high acceleration gradient, which is directly adjacent to the photocathode. Such sources are required to form clumps with a charge of a few nC at a small emittance of a few mm·mrad. These requirements are contradictory to some extent, in this connection it seems relevant to study in detail the basic parameters of the gun for emittance formation. T. Rao and D. Dowell [11] discuss the theoretical basis, numerical modeling methods, and technology for conventional and superconducting photoinjectors. J. Hahn's thesis [12] and paper [13] discuss dark currents and multipactor effects in photocannon. The paper by J. Hahn et al. [14] is devoted to the study of the influence of secondary emission in the photocathode region on the beam quality. The analytic theory of photocannon by L. Serafini and J. Rosenzweig [15] considers the dynamics of the beam contour and emittance in the paraxial approximation.

The problem of using adequate mathematical methods and computer programs was posed in a paper [16] in 2005. There, the available programs available at that time were compared on model problems: the commercial code MAGIC, V. Ivanov's MAXWELL-T program package, and the Parmela program developed at Los Alamos National Laboratory. The first two programs solve the system of Maxwell's equations to calculate electromagnetic fields and use the particle-in-cell method to calculate particle dynamics. They have shown on model problems that the results of the calculation of the transverse emittance of clusters match with an accuracy of 1–2%, while the results of the Parmela program, which is widely used to calculate the dynamics of beams in gas pedals, showed a difference of the order of 10%. It was

found that the reason for such a significant difference is that this program does not take into account the azimuthal component of the intrinsic magnetic field of the relativistic beam, so the use of this program for the calculation of photocannons with small emittance is not recommended. The photocannon used in the high-power X-ray free-electron laser at the Stanford Linear Accelerator Center [17] was further developed on the basis of these calculations.

The photocannon design process can be divided into two phases. At the first stage, the optimal modes of operation are selected, i.e., the parameters of the high-frequency field of the resonant cavities, the quasi-stationary Coulomb field of the clots, the parameters of the laser pulse, the accompanying stationary external magnetic field, etc. are matched. For this purpose, one can use simplified numerical and analytical models, such as those described in the works of K. Kim [6] and L. Serafini [15], which allow one to obtain numerical solutions in a few seconds of machine time. Only after optimization problems are solved can calculations be performed using more powerful and more accurate methods and programs that allow the investigation of subtle physical effects. Such universal programs are, for example, CST Microwave Studio, GdFidI, and dr. Calculations for these programs can take several hours. The reason is that universal programs, as a rule, do not take into account the specifics of physical processes in photocannons. These shortcomings were addressed in the developments at MEFHI, where a series of 2D and 3D programs with the common name BEAMDULAC were created. Each version of this program is oriented to the calculation of a specific problem statement and allows to simulate the dynamics of electron, ion beams and mixtures of particles with different charges and masses. The algorithms of these programs are based on the use of fast Fourier transform methods to calculate the quasi-static Coulomb fields of clots and the cloud-in-cell method to calculate the particle dynamics [18–20].

In the present paper, we consider a more limited physical model using a numerical and analytical approach. In the case of a small cluster charge, the determining factor in the formation of transverse emittance is the accelerating field of the RF resonant cavity, which makes it possible to analyze the dynamics of emittance in the paraxial approximation analytically. For a clot with a charge of a few nC the Coulomb field of the clot becomes dominant. In this case, the analytical technique can be used only in the ultra-relativistic energy region under additional assumptions concerning the shape of the cluster, its size, and the charge density distribution, and at the stage of its acceleration from the photocathode it is necessary to use numerical models to calculate the beam dynamics.

Generally speaking, the final values of the longitudinal and transverse emittances of the clots formed under the influence of the high-frequency field of resonant cavities and Coulomb fields are not a simple sum of separate contributions, as is the case in the algorithms of the ASTRA

program. Our goal is to obtain quantitative criteria for the dependence of emittance under the propagating action of Coulomb fields alone for subsequent comparison with the effect of RF fields on beam emittance.

## 1. Accounting of Coulomb fields of the charged clot

The propagating effect of the Coulomb fields of a cluster of electrons is usually considered in a coordinate system moving with the center of the cluster. In this case, it is assumed that the clot is monoenergetic, i.e., all particles of the clot move with the same velocity  $v$ , determined by a high-frequency field with amplitude  $E_z$ . In this system, the components of the electromagnetic field — are purely electrostatic  $(E'_x, E'_y, E'_z)$ . The reverse transition to the laboratory system leads to the appearance of the intrinsic magnetic field of the beam, which is directly related to the electrostatic field in the moving coordinate system by means of the correcting relativistic factor. After analyzing the dynamics, we can proceed to the laboratory system using the inverse Lorentz transformation

$$E_x = \gamma E'_x, \quad B_y = \gamma \frac{v}{c^2} E'_x, \quad E_z = E'_z.$$

In further calculations, for simplicity, we will omit the stroke symbols relating to the moving system. We will take the dependence of  $\gamma(z)$  of the relativistic factor on the longitudinal coordinate from the analysis of the longitudinal dynamics of the cluster, which is the subject of a separate publication.

The potential  $\varphi(u)$  of a clot is determined by integrating its charge density  $\rho(s)$  over the volume of the clot  $V$ :

$$\varphi(u) = \frac{1}{4\pi\epsilon_0} \int_V \frac{\rho(s)}{R_{us}} dV, \quad s \in V, \quad (1)$$

where  $R_{us}$  — the distance between the observation point  $u$  and the field source point  $s$ ,  $\epsilon_0$  — the dielectric constant of vacuum.

### 1.1. Cylindrical clot with homogeneous charge distribution

Assuming that the charge distribution of the clot is homogeneous, the charge density  $\rho$  can be taken beyond the integral sign, replacing it by the total charge divided by the clot volume  $Q/V$ . Next, we need to make an assumption about the shape of the clot. For a homogeneous distribution of the volume charge one can consider clots of different shapes, including arbitrary three-dimensional ones. Consider a uniformly charged cylinder of radius  $R_b$  of length  $L_b$ , whose center is located at the origin. Clot volume  $V = \pi R_b^2 L_b$ . Integrating by the azimuthal variable

of the cylindrical coordinate system  $(r, z, \theta)$ , we obtain an expression for the potential (see [21])

$$\varphi_b(r, z) = \frac{Q}{\pi V \epsilon_0} \int_0^{R_b} r' dr' \int_{-L_b/2}^{+L_b/2} dz' \frac{K(t)}{A},$$

$$A^2 = (r + r')^2 + (z - z')^2. \quad (2)$$

Here  $K(t)$  — the full elliptic integral of 1st kind,  $t = 2 \frac{\sqrt{rr'}}{A}$ . By differentiation of the potential we obtain the electric field components

$$E_{r,b}(r, z) = \frac{Q}{2\pi r V \epsilon_0} \int_0^{R_b} r' dr' \int_{-L_b/2}^{+L_b/2} dz' \times \frac{1}{A} \left[ K(t) - E(t) \frac{(r')^2 - r^2 + (z - z')^2}{(r - r')^2 + (z - z')^2} \right] dz', \quad (3)$$

$$E_{z,b}(r, z) = \frac{Q}{\pi V \epsilon_0} \int_0^{R_b} r' dr' \int_{-L_b/2}^{+L_b/2} dz' \frac{(z - z')E(t)}{A[(r - r')^2 + (z - z')^2]}. \quad (4)$$

Here  $E(t)$  — the complete elliptic integral of genus 2. Both integrals can be approximated by polynomials (see [22]):

$$E(t) = a_i \eta^i + b_i \eta^i \ln(\eta), \quad \eta = \sqrt{1 - t^2},$$

$$K(t) = c_i \eta^i + d_i \eta^i \ln(\eta).$$

4th degree polynomials are sufficient to calculate integrals to within ten correct signs.

In fact, the potential and electric field are time dependent. This dependence is determined by the fact that the clot flies along the axis  $z$  with velocity  $v$ , so the limits of integration should be replaced by  $L_b + vt$  after the transition to the laboratory system. If the clot has not completely exited the cathode, the length of the clot  $L_b$  will not be constant at the initial time instants, but its field at each time instant will be calculated by the same formulas (2)–(4). In the calculations below, the amplitude of the fields will increase smoothly at the initial moments of time from the initial value corresponding to the fields in the absence of a clot to the maximum values shown in the figures below.

The radial component of the electric field will be the sum of the high frequency field  $E_r$  and the clot field  $E_{r,b}$ . The calculation of the azimuthal component of the intrinsic magnetic field of the relativistic cluster we obtain in a similar way. This component is related to the radial force, which partially compensates for the Coulomb pushing force because it contributes to the Lorentz force  $[v \times B]$  of opposite sign to the pushing force. In laboratory system it has the form

$$B_{\theta,b}(u) = \frac{\mu_0}{4\pi} \int_V \frac{[j_z(s) \times R_{us}]}{R_{us}^3} dV, \quad s \in V, \quad (5)$$

where  $\mu_0$  — magnetic constant of vacuum,  $j_z$  — clot current density,  $V$  — volume occupied by clot currents.

Since the external magnetic field is stationary, in the laboratory coordinate system it should simply be added to the calculated fields of the clot when calculating the emittance.

The expressions (2)–(4) for the potential and electric field components can be easily generalized to the case of arbitrary charge distribution and arbitrary clot shape. This requires bringing the charge density distribution under the sign of the integral and replacing the limits of integration on the variables  $r$  and  $z$ , so that they vary within the volume of the clot.

The maximum influence of the Coulomb fields on the particle dynamics should be expected near the photocathode, where the electric field of the clot makes a significant contribution to the transverse motion. In order to account for the influence of the electrodes on the self-consistent electric field, it is necessary to solve the boundary value problem for the Poisson equation with boundary conditions at all electrodes. In fact, strict consideration of boundary conditions is necessary only when the distance from the center of the clot to the boundary is comparable to the size of the clot itself. At larger distances, it is sufficient to consider the total field as the sum of the fields of the electrodes and the clot in the space free of charges. In our case, we will use a simple model with a flat cathode. Then the radial component of the total electric field  $E_{rs}$  at the cathode must be equal to zero. This condition is automatically satisfied if one considers the field of a mirrored clot with opposite charge sign on the other side of the cathode  $E_{rs} = E_{r,b}(r, z) - E_{r,b}(r, -z)$ . As the clot moves away from the cathode, the radial field will increase and the field of the mirrored clot will decrease. The most difficult for analyzing the dynamics of emittance formation is the region of acceleration of the cluster from the photocathode to the region of relativistic energies. When the clot is formed by a laser pulse, this region is not too extended, but in this region the effect of Coulomb fields can be studied only numerically [17]. In our further calculations we will give data for the Coulomb fields in the laboratory system, where the transverse components of the Lorentz force decrease with respect to the moving coordinate system, taking into account the coefficient  $1/\gamma^2(z)$ , due to the compensating effect of the beam's own magnetic field on the radial force.

The advantages of the presented approximate model are that it does not require the use of such complicated programs as GPT [23] or Astra [24], which solve problems by the macroparticle method, but is limited to the calculation of simple integrals, and at the same time allows us to calculate the fields and beam emittance with an acceptable accuracy for practice.

A number of assumptions are made in the model under consideration. The single direct and inverse Lorentz transformations are possible only for a monoenergetic beam with the same velocities for all particles. This is possible if

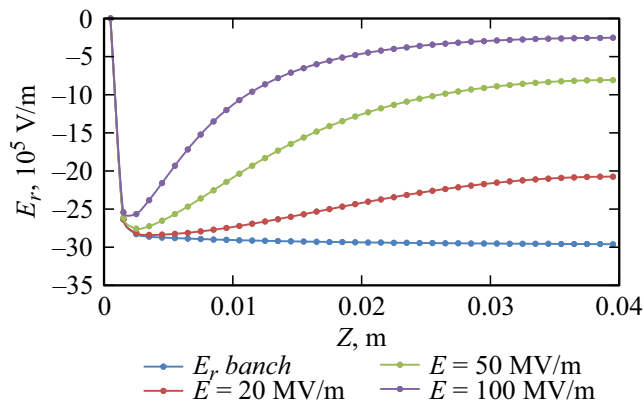


**Figure 1.** Radial component of the total field  $E_{r,s}$  for a cylindrical clot of diameter 2.5 mm, length 1 mm, with uniformly distributed charge 1.5 nC without taking into account the intrinsic magnetic field (blue line (online version)) and taking into account this field for different values of the accelerating field  $E$  in the laboratory coordinate system.

the characteristic size of the cluster is much smaller than the wavelength of the high-frequency field, which determines the dynamics of the particles. Since the particles are effectively accelerated in the near-cathode part, operation with the proposed model for a cluster partially exiting the photocathode is possible if the exiting cluster is broken along the  $z$  axis into fragments for which the particles can be considered monoenergetic with the required accuracy. The fields for each of these fragments should be counted separately and then summarized.

Analysis of the data presented in Fig. 1 shows that at high gradients of the accelerating fields, the influence of Coulomb fields on the dynamics of transverse emittance formation is significant only in the non-relativistic region of beam motion, which takes place in the first resonant cavity adjacent to the photocathode.

It can be seen that the radial component of the total field is strictly equal to zero at the cathode, monotonically increases as the clot moves away from the cathode, reaches a maximum, and then monotonically decreases due to the contribution of the magnetic field of the clot.

### 1.2. Cylindrical clot with Gaussian distribution

Consider also the case of a clot with a Gaussian volume charge distribution

$$f(x) = \frac{1}{\sqrt{2\pi}\sigma} \exp\left[-\frac{1}{2}\left(\frac{x-M}{\sigma}\right)^2\right], \quad (6)$$

where  $\sigma$  — the half-width of the distribution, and  $M$  — the mean of the distribution.

Setting the characteristic dimensions of the clot  $\sigma_r$  and  $\sigma_z$ , in formulas (1) – (3) we replace the value  $Q/V$  by the charge density  $\rho(r, z)$ , bringing it under the sign of the integral. Since 99% of the distribution area (6) is in the

coordinate range  $z(-3\sigma, 3\sigma)$ , the length of the clot should be increased by a factor of 6 times and its radius — by a factor of 3 times to compare with the previous results. In our case, the mean value of  $M_r = 0$ , and  $M_z$  corresponds to the  $z$  coordinate of the clot center. The distribution of Coulomb fields for this case is presented in Fig. 2.

Here the reduction of the radial component of the Coulomb field is an order of magnitude smaller with respect to the case of a homogeneous charge distribution. This is explained by the fact that the curves in Fig. 1, 2 correspond to the field action on the outermost particles having the maximum radius. They are affected by the full charge  $Q$ . For a Gaussian distribution, this distance is  $3\sigma_r$ , and the radial field declines as the inverse square of the radius. The dependence of the Coulomb fields on the charge of the cylindrical clot for the accelerating field  $E = 100$  MV/m is shown in Fig. 3.

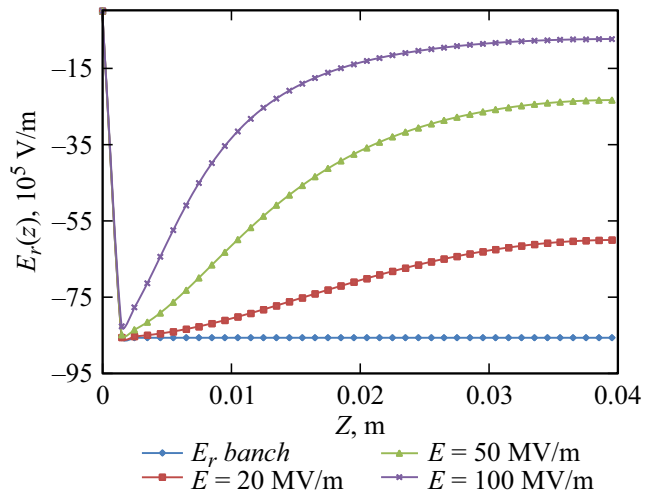


**Figure 2.** Radial Coulomb field of a cluster with Gaussian charge distribution of magnitude  $Q = 1.5$  nC for different values of the accelerating field  $E$ .

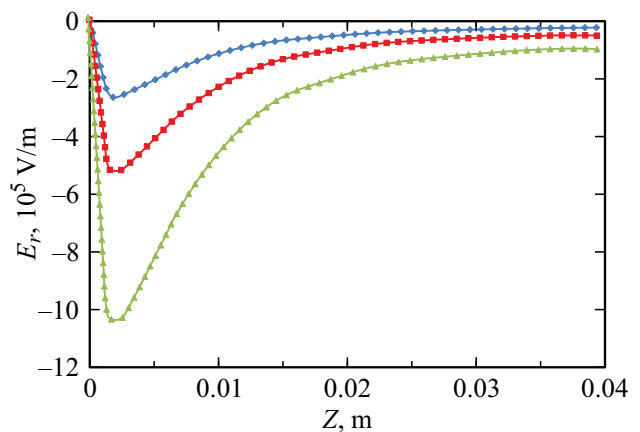


**Figure 3.** Radial component of the Coulomb field of a cylindrical clot with uniform charge distribution  $Q = 1.5$  nC — blue line (in online version), 3 nC — red line (in online version), 6 nC — green line (in online version).

### 1.3. A clot of arbitrary three-dimensional shape

Since the laser irradiates the photocathode surface at some angle to the axis of symmetry, and the center of the laser spot on the photocathode may deviate from this axis determined by the configuration of the high-frequency field of the resonant cavity, the clot generated by the laser pulse may have a shape other than axisymmetric. The transverse dynamics of such clots and its influence on emittance formation have not been investigated before.

Under certain assumptions, the field characteristics of a cluster of arbitrary three-dimensional shape can be calculated analytically. Such a result for two-dimensional distributions in Cartesian and cylindrical coordinates with a bilinear charge density distribution was obtained in [25]. J. Kwang et al. published a similar result for three-dimensional beams with a piecewise constant approximation of the charge density [26]. Such approximation gives a significant error in calculations of the field parameters, especially at the cluster boundary, which is absolutely inadmissible in calculations of the beam emittance. A much more accurate algorithm is proposed in the article by V. Ivanov [27].

Consider an irregular parallelepipedal grid in Cartesian coordinates  $\{x_i\} \times \{y_j\} \times \{z_k\}$  with a linear approximation of the charge density on each variable:

$$\begin{aligned} \rho(x, y, z) = & \left\{ \left[ (\rho_{i+1,j,k}(x - x_i) + \rho_{i,j,k}(x_{i+1} - x)) \right. \right. \\ & \times (y_{j+1} - y) + (\rho_{i+1,j,k}(x - x_i) + \rho_{i,j,k}(x_{i+1} - x)) \\ & \times (y - y_j) \left. \right] (z_{k+1} - z) + \left[ (\rho_{i+1,j,k}(x - x_i) \right. \\ & + \rho_{i,j,k}(x_{i+1} - x))(y_{j+1} - y) + (\rho_{i+1,j,k}(x - x_i) \\ & + \rho_{i,j,k}(x_{i+1} - x))(y - y_j) \left. \right] (z - z_k) \left. \right\} / [(x_{i+1} - x_i) \\ & \times (y_{j+1} - y_j)(z_{k+1} - z_k)]. \end{aligned} \quad (7)$$

To calculate the potential at the point  $(x_0, y_0, z_0)$ :

$$\varphi(x_0, y_0, z_0) = \frac{1}{4\pi\epsilon_0} \sum_{i,j,k} \int_{x_i}^{x_{i+1}} \int_{y_j}^{y_{j+1}} \int_{z_k}^{z_{k+1}} \frac{\rho(x, y, z)}{R} dx dy dz, \quad (8)$$

it is necessary to calculate four moments of charge density

$$\begin{aligned} J_1 = \iiint \frac{x}{R} dx dy dz, \quad J_2 = \iiint \frac{xy}{R} dx dy dz, \\ J_3 = \iiint \frac{xyz}{R} dx dy dz, \quad J_4 = \iiint \frac{1}{R} dx dy dz, \end{aligned} \quad (9)$$

where  $R = \sqrt{(x - x_0)^2 + (y - y_0)^2 + (z - z_0)^2}$ . The remaining integrals are obtained by cyclic substitution of the variables  $x, y, z$ .

After replacing  $\tilde{x} = x_0 - x, \tilde{y} = y_0 - y, \tilde{z} = z_0 - z$  and  $r^2 = x^2 + y^2 + z^2$ , all integrals are calculated analytically

$$\begin{aligned} J_1 = & \frac{y}{4} [yz + (x^2 + y^2) \ln |z + r|] + \frac{z^3}{6} \ln |y + r| \\ & + \frac{x^2}{2} \left[ z \ln |y + r| + y \ln |z + r| - z + x \tan^{-1} \left( \frac{z}{x} \right) \right. \\ & - x \tan^{-1} \left( \frac{zy}{xr} \right) \left. \right] + \frac{1}{36} \left\{ 6x^2z - 2x^3 + 6x^3 \left[ \tan^{-1} \left( \frac{z}{x} \right) \right. \right. \\ & \left. \left. - \tan^{-1} \left( \frac{zy}{xr} \right) \right] - 3y(y^2 + 3x^2 \ln |z + r|) \right\}, \\ J_2 = & \frac{zr^3}{12} + \frac{3}{24} (x^2 + y^2) [zr + (x^2 + y^2) \ln |z + r|], \\ J_3 = & \frac{r^5}{15}, \end{aligned}$$

$$\begin{aligned} J_4 = & xy \ln |z + r| + yz \ln |x + r| + zx \ln |y + r| \\ & - \frac{1}{2} \left[ x \tan^{-1} \left( \frac{zy}{xr} \right) + y \tan^{-1} \left( \frac{zx}{yr} \right) + z \tan^{-1} \left( \frac{xy}{zr} \right) \right]. \end{aligned}$$

To calculate the field gradients, the obtained integrals should be differentiated by the corresponding coordinate of the observation point. Thus, for example, for the field component  $E_z$ , we obtain the following integrals:

$$\begin{aligned} J_{1z} = & \iint \frac{dx dy}{r} \\ & = -z \tan^{-1} \left( \frac{xy}{zr} \right) + y \ln |x + r| + x \ln |y + r|, \\ J_{2z} = & \iint \frac{xdx dy}{r} = \frac{1}{2} [yr + (x^2 + y^2) \ln |y + r|], \\ J_{3z} = & \iint \frac{zdx dy}{r} = zJ_{1z}, \quad J_{4z} = \iint \frac{xy dx dy}{r} = \frac{r^{3/2}}{3}, \\ J_{5z} = & \iint \frac{xz dx dy}{r} = zJ_{2z}, \quad J_{6z} = \iint \frac{xyz dx dy}{r} = \frac{z}{3} r^{3/2}. \end{aligned}$$

The remaining integrals are obtained by cyclic substitution of the variables  $x, y, z$ . Particular attention should be paid to the problem of calculating singularities at the beam boundary [17], since inaccurate accounting of singularities leads to a significant error in the calculation of the beam contour, as is the case, for example, for the piecewise constant approximation of the volume charge. An efficient analytical model for the calculation of three-dimensional Coulomb fields in photocannons is presented for the first time.

## 2. Formation of beam emittance

In further consideration, we will follow the ideas set forth in K.-J. Kima [6]. We introduce a scaling factor  $A = \sigma_r / \sigma_z$  for a clot with characteristic dimensions  $\sigma_r, \sigma_z$ , allowing us to separate a thin disk with  $A > 1$  from a long cigar-shaped

clot with  $A < 1$ . Normalized emittance is defined by the formula

$$\epsilon_s = \sqrt{\langle s^2 \rangle \langle p_s^2 \rangle - \langle s p_s \rangle^2}, \quad (10)$$

where the index  $s = r$  corresponds to transverse emittance and  $s = z$  — longitudinal.

Introducing the dimensionless parameter

$$\tau = \frac{eE_0}{2mc^2k} \quad (11)$$

and normalized field of spatial charge  $E_{sc}$ , using the formula

$$E_{sc}(x, y, z_0) = \frac{n_0}{4\pi\epsilon_0} \tilde{E}(x, y, z_0), \quad (12)$$

we can obtain an expression for emittance in the form [6]

$$\epsilon_s = \frac{\pi}{4\tau k \sin(\varphi_0)} \frac{I}{I_a} \mu_s(A). \quad (13)$$

Here,  $k$  — wave vector,  $\varphi_0$  — initial phase of the cluster,  $z_0$  — axial coordinate of the cluster center,  $n_0$  — linear charge density of the cluster in the axial direction,  $I$  — cluster current amplitude,  $I_a$  — Alfvén current, and the dimensionless function

$$\mu_s(A) = \sqrt{\langle s \rangle^2 \langle \tilde{E}_s \rangle^2 - \langle s \tilde{E}_s \rangle^2} \quad (14)$$

reflects the dependence of emittance on the shape of the clot and its field.

For a Gaussian distribution

$$\rho(x, y, z_0) = \rho_0 \exp \left[ -\frac{1}{2} \left( \frac{x^2 + y^2}{\sigma_x^2} + \frac{z_0^2}{\sigma_z^2} \right) \right], \quad (15)$$

where  $\rho_0$  — charge density in the center of the cluster, the dimensionless function of the form  $\mu_s$  is represented by the integrals

$$\begin{aligned} \mu_r^2(A) = & \int_0^\infty d\xi_1 \int_0^\infty \left\{ \frac{1}{[(1 + \xi_1)(1 + \xi_2) + 2 + \xi_1 + \xi_2]^2} \right. \\ & \times \frac{1}{\sqrt{(1 + A^2\xi_1)(1 + A^2\xi_2) + 2 + A^2\xi_1 + A^2\xi_2}} d\xi_2 \\ & \left. - \left[ \int_0^\infty d\xi \frac{1}{(2 + \xi)^2 \sqrt{2 + \xi A^2}} \right]^2 \right\}, \quad (16) \end{aligned}$$

$$\begin{aligned} \mu_z^2(A) = & \int_0^\infty d\xi_1 \int_0^\infty \left\{ \frac{1}{(A^2 + \xi_1)(A^2 + \xi_2) + 2A^4 + (\xi_1 + \xi_2)A^2} \right. \\ & \times \frac{1}{[(1 + \xi_1)(1 + \xi_2) + 2 + \xi_1 + \xi_2]^{3/2}} d\xi_2 \\ & \left. - \left[ \int_0^\infty d\xi \frac{1}{(2A^2 + \xi)^2 (2 + \xi)^{3/2}} \right]^2 \right\}. \quad (17) \end{aligned}$$

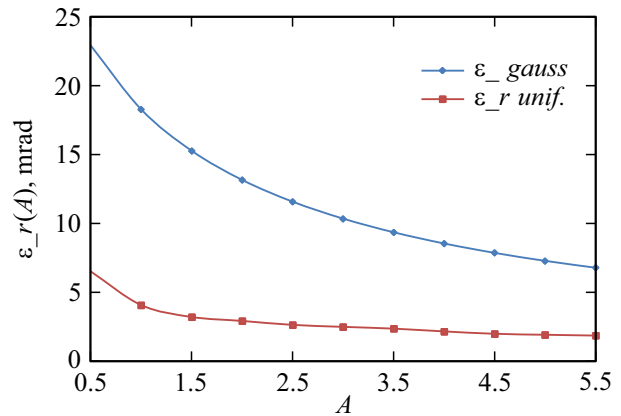


**Figure 4.** Dependence of the transverse emittance of a cylindrical beam on the  $A = R/L$  parameter for Gaussian (blue line (online version)) and homogeneous (red line (online version)) charge density distributions.

The shape function — is a universal characteristic that defines the dependence of emittance on clot shape for a particular clot charge density distribution. This function will be different for different types of density distributions. For a cylindrical clot of radius  $R$ , length  $L$  with homogeneous charge distribution  $\langle r^2 \rangle = R^2/4$ , the normalized fields are defined by the formulas

$$\tilde{E}_r(x, y, z) = \frac{2x}{\pi r R} \int_0^\pi \cos(\varphi) \log \frac{R_- - z_-}{R_+ - z_+} d\varphi, \quad (18)$$

$$\begin{aligned} \tilde{E}_z(x, y, z) = & \frac{2}{\pi R^2} \int_0^\pi d\varphi \left\{ R_- - R_+ \right. \\ & \left. + \sqrt{r^2 + z_+^2} - \sqrt{r^2 + z_-^2} + r \cos(\varphi) \right. \\ & \left. \times \log \frac{-r \cos(\varphi) + \sqrt{r^2 + z_+^2} (R - r \cos(\varphi) + R_-)}{-r \cos(\varphi) + \sqrt{r^2 + z_-^2} (R - r \cos(\varphi) + R_+)} \right\}, \\ & r^2 = x^2 + y^2, \quad R_\pm^2 = R^2 + r^2 - 2Rr \cos(\varphi) + z_\pm^2, \\ & z_\pm = z + L/2, \quad (19) \end{aligned}$$

and the form function for calculating the emittance has the form

$$\mu_s(A) = \sqrt{\langle \tilde{E}_s^2 \rangle \langle s^2 \rangle - \langle s \tilde{E}_s \rangle^2}. \quad (20)$$

Calculations of the transverse emittance of a cylindrical clot with a Gaussian charge distribution of size  $Q = 1.5$  nC, radius  $R = 1$  mm under an accelerating field of amplitude  $E_0 = 70$  MV/m are presented in Fig. 4. Similar data for longitudinal emittance are shown in Fig. 5. The results of our calculations are in good agreement with the publications [6,7].

As an example of a three-dimensional problem, we consider a clot in the form of a triaxial ellipsoid with a Gaussian charge density distribution along the axes

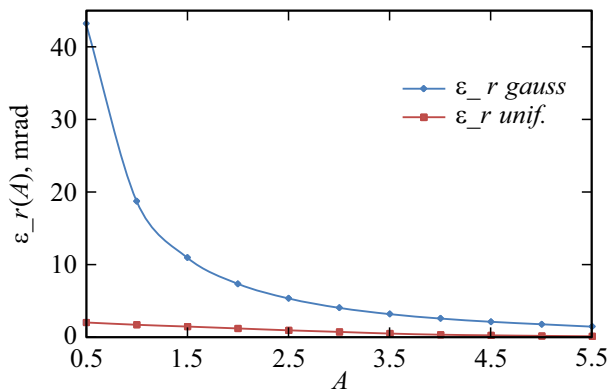


**Figure 5.** Dependence of the longitudinal emittance of a cylindrical beam on the  $A = R/L$  parameter for Gaussian (blue line (online version)) and homogeneous (red line (online version)) charge density distributions.

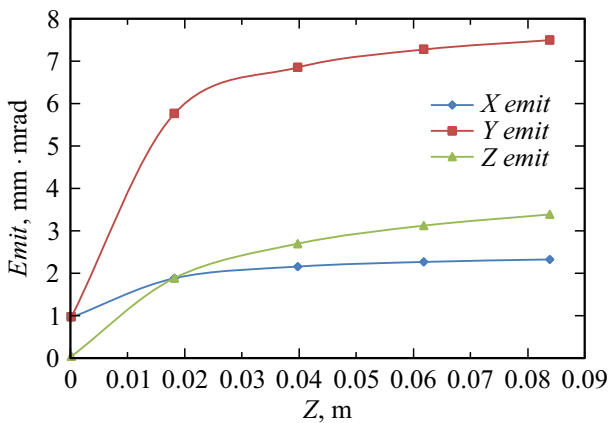


**Figure 6.** Vertical, horizontal and longitudinal emittances of a three-dimensional shaped clot

$\sigma_x = 0.5$  cm,  $\sigma_y = 1$  cm,  $\sigma_z = 2$  cm, initial transverse emittance 1 mm·mrad. The longitudinal and transverse emittances are shown in Fig. 6. The spatial charge is approximated by cubic cells of size 0.25 mm. With accounting for three planes of symmetry by  $x$ ,  $y$  and  $z$  the total number of cells was 12 000 cells, which represented an elliptically shaped clot.

### 3. Comparison of the proposed model with other approaches

The limitation of the semi-analytic theory proposed by K. Kim [6] is that it considers only cylindrical clots with homogeneous or Gaussian charge distribution. In addition, this model does not take into account the field of mirror-reflected charges in the vicinity of the emitter, so the normalized clot fields do not satisfy the exact boundary conditions on the cathode surface. Our proposed model is free from these drawbacks.

Another approach is implemented in the fully numerical algorithms of the Astra and CST Microwave Studio packages. Here the spatial charge is represented by macroparticles, which makes it possible to take into account many special physical phenomena in the formulation of the problem, but requires the use of tens and hundreds of thousands of macroparticles to obtain smooth distributions for the field and emittance of clots. In addition, the Astra program requires input of characteristics of electric and magnetic fields calculated by other programs. Moreover, in this approach, the addition of external fields, in general, does not guarantee self-consistency of the total field satisfying all boundary conditions of the problem, although it takes into account the field of mirror charges in the vicinity of the cathode. By definition, the self-consistent field is the total field of the beam and external sources (electrodes, solenoids, permanent magnets) satisfying the boundary conditions of the problem. Here, external fields mean fields calculated by external programs, and internal — beam fields calculated by the program „Astra“. When setting the particle emission mode (Cathode = T), the program ensures that the first-order boundary condition for the potential at the cathode is equal to zero by adding mirror-reflected charges of opposite sign to the left of the cathode, i.e., it does the same thing as the authors do in their algorithm. Correctly calculated external fields input from external files must also give zero values at the cathode so that the total field potential at the cathode remains zero. The words „in the general case does not guarantee self-consistency of the total field“ mean that when calculating the beam dynamics by the program „Astra“ the sum of the external fields and the beam fields will satisfy the conditions of the boundary value problem only in the vicinity of the cathode, but not at the other electrodes. If the other electrodes are located far enough from the beam, the violation of the boundary conditions and their influence on the beam dynamics will be negligible. However, if the beam approaches close enough to the aperture, this influence is no longer small.

The CST Microwave Studio package implements a technique for solving the initial boundary value problem for the system of Maxwell's equations with the particle-in-cell method, but careful consideration of the boundary conditions for the external and intrinsic fields of the particles imposes very serious limitations on the amount of computational resources — required memory and time to solve the problem. The results of our calculations of the transverse emittance of a cylindrical clot with an initial emittance at the cathode of 0.5 mm·mrad and a clot charge of 1.5 nC for a field at the cathode of 70 MV/m are in good agreement with the calculations using the Astra program, but require two orders of magnitude less counting time and computer memory.

The results of calculations of transverse emittance for a cylindrical clot with homogeneous charge density distribution, initial emittance at the cathode of 0.5 mm·mrad and total charge of 1.5 nC at a field strength at the cathode of 70 MV/m according to the proposed model are presented



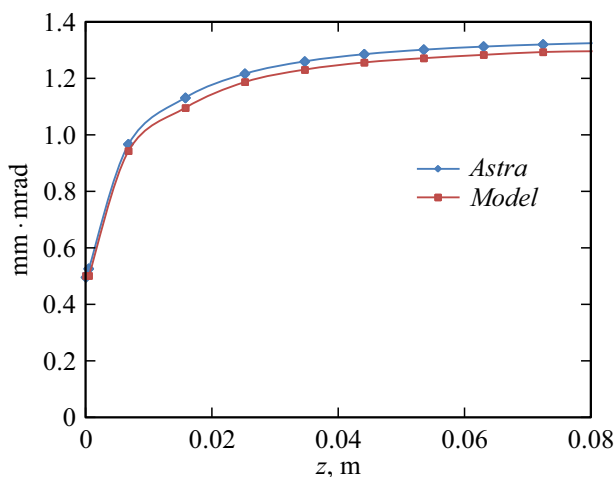


**Figure 7.** Transverse emittance of a cylindrical cluster with homogeneous charge density distribution calculated by numerical-analytical model and with the program „Astra“.

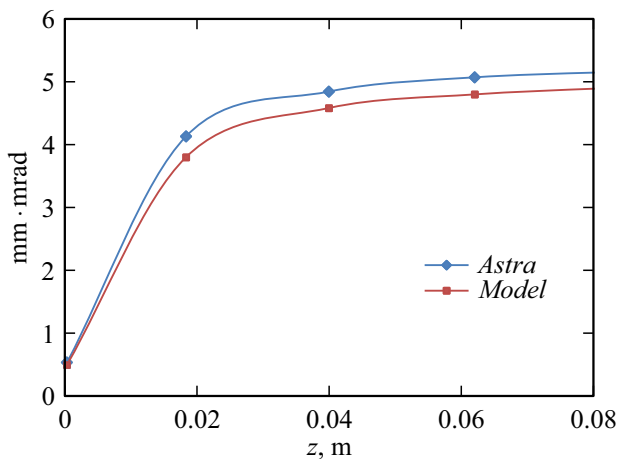


**Figure 8.** Transverse emittance of a cylindrical cluster with a Gaussian charge density distribution calculated by the numerical-analytical model and with the program „Astra“.

in Fig. 7. For similar configurations, the clot was modeled with 50 thousand macroparticles using the Astra program; the computation time was 19 min, while calculations using the proposed semi-analytical model took 5 s. A comparative analysis of the same problem with a Gaussian charge density distribution is shown in Fig. 8.

## Conclusion

The performed theoretical analysis and numerical calculations give a clear understanding of the role of Coulomb fields in the formation of emittance in photocannon. The obtained results reveal the relation of emittance not only with the geometrical dimensions and shape of the clot, but also with the parameters of the charge density distribution in the clot. It is shown quantitatively that the magnitudes of the longitudinal and transverse emittances are minimal for

a homogeneous distribution and increase significantly for Gaussian distributions in the longitudinal (by 3–10 times depending on the parameter  $A$ ) and transverse (by a factor of about three) directions. For a thin disk-shaped clot, the growth of transverse emittance can be much larger than its growth in the longitudinal direction. These numerical results can serve as a basis for comparing the degree of influence of the high-frequency field of the resonant cavities and the Coulomb fields of the clusters on the total emittance of the beam at the exit of the photocannon.

## Conflict of interest

The authors declare that they have no conflict of interest.

## References

- [1] T. Miura, M. Akemoto, D. Arakawa, Y. Arakida, A. Enomoto, S. Fukuda, Y. Funakoshi, K. Furukawa, T. Higo, H. Honma, R. Ichimiya, N. Iida, M. Ikeda, E. Kadokura, H. Kaji, K. Kakihara, T. Kamitani, H. Katagiri, M. Kurashina, S. Matsumoto, T. Matsumoto, H. Matsushita, S. Michizono, K. Mikawa, F. Miyahara, H. Nakajima, K. Nakao, T. Natsui, Y. Ogawa, Y. Ohnishi, S. Ohsawa, F. Qiu, M. Satoh, T. Shidara, A. Shirakawa, H. Sugimoto, T. Suwada, T. Takenaka, M. Tanaka, Y. Yano, K. Yokoyama, M. Yoshida, L. Zang, X. Zhou. *Upgrade Status of Injector LINAC for SuperKEKB*, in Proc. IPAC'14 (Dresden, Germany, 2014), p. 59–61.
- [2] Electronic source. Available at: <https://www-linac.kek.jp/linac-com/report/b2gm/linac-status-satoh-200622.pdf>
- [3] Electronic source. Available at: <https://link.springer.com/content/pdf/10.1140/epjst/e2019-900045-4.pdf>
- [4] Electronic source. Available at: <https://ctd.inp.nsk.su/c-tau/>
- [5] D. Nguyen, J. Lewellen, L. Duffy. *RF Linac for High-Gain FEL. Photoinjectors*, US (Particle Accelerator School, June 16–20, 2014) [https://uspas.fnal.gov/materials/14UNM/B\\_Photoinjectors.pdf](https://uspas.fnal.gov/materials/14UNM/B_Photoinjectors.pdf)
- [6] K.-J. Kim. *NIM A*, **275**, 201 (1989).
- [7] T. Natsui, M. Yoshida, X. Zhou, Y. Ogawa. *Quasi-traveling wave gun and beam commissioning for SuperKekb*. Proc. IPAC2015 (Richmond, VA, USA), p. 1610–1612.
- [8] H. Bluem, A.M.M. Todd, M.D. Cole, J. Lewellen, L. Phdlips, J. Preble, J. Rathke, T. Schultheiss. *Electron Injectors for Next Generation X-Ray Sources*, SPIE 49th Annual Mtg. (Denver, CO, 206 August, 2004)
- [9] D.H. Dowell, J.F. Schmerge. *Phys. Rev. Special Topics Accelerators and Beams*, **2**, 074201 (2009). DOI: 10.1103/PhysRevSTAB.12.074201
- [10] D. Filippetto, P. Musumeci, M. Zolotarev, G. Stupakov. *Phys. Rev. Special Topics, Accelerators and Beams*, **17**, 024201 (2014).
- [11] T. Rao, D.H. Dowell. *An Engineering Guide to Photoinjectors* (arXiv:1403.7539, 2013), 335 p.
- [12] J.-H. Han. *Dynamics of Electron Beam and Dark Current in Photocathode RF Guns* (Hamburg, 2005) [DESY-Thesis-2005-038].
- [13] J.-H. Han, K. Flöttmann, W. Harting. *Phys. Rev. Special Topics Accelerators and Beams*, **11**, 013501 (2008).



- [14] J.-H. Han, M. Krasilnikov, K. Flöttmann. *Phys. Rev. Special Topics Accelerators and Beams*, **8**, 033501 (2005).
- [15] L. Serafini, J.B. Rosenzweig. *Phys. Rev. E*, **55** (6), 7565 (1977).
- [16] E. Colby, V. Ivanov, Z. Li, C. Limborg. *Simulation Issues for RF Photoinjectors* (SLAC-PUB-11494, Sep 26, 2005), 10 p.
- [17] J.B. Rosenzweig, N. Majernik, R.R. Robles, G. Andonian, O. Camacho, A. Fukasawa, A. Kogar, G. Lawler, J. Miao, P. Musumeci, B. Naranjo, Y. Sakai, R. Candler, B. Pound, C. Pellegrini, C. Emma, A. Halavanau, J. Hastings, Z. Li, M. Nasr, S. Tantawi, P. Anisimov, B. Carlsten, F. Krawczyk, E. Simakov, L. Faillace, M. Ferrario, B. Spataro, S. Karkare, J. Maxson, Y. Ma, J. Wurtele, A. Murokh, A. Zholents, A. Cianchi, D. Cocco. *Ultra-Compact X-Ray Free-Electron Laser* (arXiv: 2003.06083v3 [physics.acc-ph] 14 Aug, 2020)
- [18] S.M. Polozov. *Nelineynaya dinamika puchkov ionov i elektronov v lineynykh uskoritelya* (Cand. diss. M., 2019), 363 p.
- [19] T.V. Bondarenko, E.S. Masunov, S.M. Polozov. *Voprosy atomnoy nauki i tekhniki*, **6** (88), 114 (2013) (in Russian).
- [20] S.M. Polozov, T.V. Bondarenko. *Beam dynamics simulation in two versions of new photogun for FCC-EE electron injector linac*. Proc. IPAC 2017 (Copenhagen, Denmark, 2017)
- [21] V.Ya. Ivanov. *Avtomatizirovannoye proyektirovaniye priborov elektroniki* (Institute of Mathematics SB RAS, Novosibirsk, 1986), Part 1. (In Russian)
- [22] C. Hastings, J. Hayward. *Approximation for Digital Computers* (Princeton, USA, 1955)
- [23] GPT: General Particle Tracer, Version 2.82, Pulsar Physics, <http://www.pulsar.nl/gpt/>
- [24] K Flöttmann. *ASTRA-Manual\_V3* [Online]. Available: FTP: <http://www.desy.de> Directory: `m̃pyflo/Astra_dokumentation/` File: `ASTRA-Manual_V3.pdf`.
- [25] V.A. Ivanov. *Metod analiza trekhmernykh nestatsionarnykh zadach dlya puchkov zaryazhennykh chastits*. Tr. of the Institute of Mathematics (Nauka, Novosibirsk, 1989), pp. 172–187. (In Russian).
- [26] J. Quang, S. Lidia, R. Ryne, C. Limborg-Deprey. *Phys. Rev. Special Topics Accelerators and Beams*, **9**, 44204 (2006).
- [27] V. Ivanov. *Int. J. Modern Phys. A*, **24** (5), 869 (2009).

*Translated by Y.Deineka*